Geophysical Prospecting, 2007, **55**, 83–89

Hankel transform filters for dipole antenna radiation in a conductive medium

F.N. Kong*

Norwegian Geotechnical Institute, PO Box 3930 Ullevaal Stadion, NO-0806 Oslo, Norway

Received November 2005, revision accepted June 2006

ABSTRACT

We discuss the Hankel transforms related to a particular application, i.e. the dipole antenna radiation in conductive media, such as the antenna radiation in sea-bed electromagnetic applications. In this application, the electromagnetic wavefields decay very rapidly with distance. A good filter means that it can be used to evaluate weak fields.

Exponential sampling transforms a Hankel transform into a convolution equation, which must be solved to obtain the filter coefficients. Here, we use a direct matrix inversion method to solve the convolution equation in the sample domain, instead of the Fourier transform method and the Wiener–Hopf method, previously used to solve the convolution equation. This direct method is conceptually simple and is suitable for our optimization process: by using the Sommerfeld identity, we search for the optimum sampling interval, which corresponds to the minimum wavefield, evaluated for a given length filter.

The performances of the new filters obtained are compared with some well-known filters. We find that our filters perform better for our application; that is, for the same length filters, our filters are able to calculate weaker fields.

For users working in similar applications, three sets of filters with lengths 61, 121, 241 are available from the author.

INTRODUCTION

To calculate the fields generated by a dipole antenna above or embedded in a layered media, we need to evaluate Hankel transforms. An efficient way of evaluating these equations is to use the digital filter technique, which was first proposed by Ghosh (1971) and later improved by Koefoed *et al.* (1972), Koefoed and Dirks (1979), Anderson (1979, 1982, 1989, 1991), Johansen and Sorensen (1979), Guptasarma (1982), Christensen (1990, 1991), Sorensen and Christensen (1994), Guptasarma and Singh (1997), and many others.

When using the digital filter technique, the Hankel transforms are first transformed into convolution equations, which are then solved to obtain the filter coefficients. Previous methods to solve the convolution equations or to perform the deconvolution can, roughly speaking, be divided into Fourier transform methods and Wiener–Hopf minimization methods.

Here, we construct the convolution equation as a matrix equation. Thus the deconvolution becomes a direct matrix-inversion problem. While constructing the matrix equation, only the input and output sample values are needed. Hence, we perform the deconvolution in the sample domain.

It is known that the determination of the digital filter is not unique. Hence, a filter, which is optimum for one application, may not be optimum for another application. In this article, the filters are used to evaluate the Hankel transforms related to the electromagnetic fields generated by a source embedded in a very conductive medium, such as those encountered in the sea-bed logging problem, etc. (Eidesmo *et al.* 2002; Ellingsrud *et al.* 2002; Kong *et al.* 2002). In this application, the fields decay very rapidly with the measurement distance. One of

*E-mail: fk@ngi.no

the important criteria defining a 'good' filter is the smallest wavefield that a particular filter can evaluate.

In the Hankel transform filter problem, there are two factors of importance. One is the evaluation accuracy, or the smallest fields which can be evaluated; the other is the length of the filter, which determines the speed with which the Hankel transform is calculated. In the sample-domain deconvolution method, the first step is to define the filter length. The sample-domain method is then suitable for the optimization procedure, i.e. searching for the optimum sampling interval to achieve the minimum wavefield evaluated for a given length filter. We use this optimization method to derive filters with three different lengths: 61, 121 and 241. These filters are compared with some known filters.

DIGITAL FILTER DESIGN

We define the Hankel transform of $p(k)$ of integer order n as

$$q(r) = \int_0^\infty p(k) \mathrm{J}_n(kr) \mathrm{d}k. \tag{1}$$

Assume $r = \mathrm{e}^{an}$ and $k = \mathrm{e}^{-am}$. We then have

$$\mathrm{e}^{an} q(\mathrm{e}^{an}) = \sum_{m=-\infty}^{\infty} p(\mathrm{e}^{-am})(\mathrm{e}^{a(n-m)} \mathrm{J}_n\left(\mathrm{e}^{a(n-m)}\right). \tag{2}$$

Equation (2) becomes a convolution equation. For the convenience of later discussions, we rewrite equation (2) in standard convolution form:

$$g(n) = \sum_{m=-\infty}^{\infty} f(m) h(n-m), \tag{3}$$

where $g(n) = \mathrm{e}^{an}\ q(\mathrm{e}^{an})$ is the known output function, $f(m) = p(\mathrm{e}^{-am})$ is the known input function, and $h(n-m) = (\mathrm{e}^{a(n-m)}\ \mathrm{J}_n(\mathrm{e}^{a(n-m)})$ is the kernel response to be determined.

The earlier methods used to solve the convolution equation or to perform the deconvolution can be divided into two categories. The first type of method has to perform deconvolution in the spectrum domain, i.e. it has to obtain the filter response in the spectrum domain by using the division of the output spectrum and the input spectrum. The filter response in the sample domain is then obtained by performing an inverse Fourier transform on the filter spectrum. According to the literature, this type of method is most frequently used.

The other type of method uses the Wiener–Hopf minimization method. This method was first introduced by Koefoed and Dirks (1979), and later improved by Guptasarma (1982) and Guptasarma and Singh (1997). The Wiener–Hopf minimization method does not need to use the spectra of the input and output functions. Instead, it uses the input and output samples directly in the sample domain, and hence it is a sample-domain method.

Here, we propose a direct method to solve the convolution equation referred to above. First, we assume that the unknown function h(n − m) has a limited length 2 L + 1 in the sample domain. From equation (3), it can be seen that for each function g(n) and the corresponding 2 L + 1-values of f, that is f(n − L) to f(n + L), we can obtain an equation. To solve the kernel response h(n − m) with 2 L + 1 unknowns, we needs 2 L + 1 equations. Analytical expressions for the functions f and g are given by equations 4 and 5 below, and we can have infinite number of known functions g(n) and f(m). Hence, it can be an overdetermined system. The Wiener–Hopf method is an optimization method to solve this overdetermined system. Here, we choose only n = −L to L to construct 2 L + 1 equations for solving the kernel response with 2 L + 1 unknowns, which can be obtained by inverting the matrix, or using the well-known synthetic division method. This is the main difference between our method and the Wiener–Hopf method.

We have chosen the following analytical Hankel transform expressions (see, e.g. Guptasarma and Singh 1997) to calculate the kernel responses, J_0 and J_1, respectively:

$$\int_0^\infty k \mathrm{e}^{-ck^2} \mathrm{J}_0(kr) \mathrm{d}k = \frac{1}{2c} \mathrm{e}^{-\frac{r^2}{4c}}, \tag{4}$$

$$\int_0^\infty k^2 \mathrm{e}^{-ck^2} \mathrm{J}_1(kr) \mathrm{d}k = \frac{r}{4c^2} \mathrm{e}^{-\frac{r^2}{4c}}, \tag{5}$$

where the value c = 3 is chosen.

The optimization procedure is as follows

(a) Choose the length of the filter and use $r = \mathrm{e}^{an}$ and $k = \mathrm{e}^{-am}$ to sample the input f(n) and output g(n) of equation (4), with the sampling interval a varying from 0.005 to 0.4 in steps of 0.005.
(b) Solve the matrix equation (3) using any matrix inversion routine, or the synthetic division method, and obtain a set of J_0 filter coefficients for each sampling interval a.
(c) Use the J_0 filters obtained to evaluate the following Sommerfeld identity (see, e.g. Equation (B5) in Appendix B of Chave and Cox 1982):

$$\int_0^\infty \mathrm{d}k \mathrm{J}_0(k\rho) \frac{k}{\beta} \mathrm{e}^{-\beta|z-z'|} = \frac{\mathrm{e}^{-\gamma R}}{R}. \tag{6}$$

Equation (6) is related to the antenna radiation in a homogeneous and conductive medium, where ρ is the radial distance, z′ is the height of the source and z is the height of the receiver. The parameters are as follows:

$$z' = 50\,\mathrm{m},$$

$$z = 0,$$

$$R = \sqrt{\rho^2 + z'^2},$$

$$\gamma = \sqrt{\mathrm{i}2\pi\mu_0 f\sigma},$$

$$\beta = \sqrt{k^2 - \gamma^2},$$

frequency f = 1 Hz,
conductivity of the medium, $\sigma = 3.2$ S/m.
For each J_0 filter, which corresponds to a sampling interval a, we calculate the smallest wavefield evaluated, and obtain a curve of the smallest field (magnitude) versus the sampling interval a.

(d) Choose the optimum sampling interval, which corresponds to the minimum of the smallest field curve. Fig. 1 shows three curves of the smallest fields for the filter length 61, 121 and 241. Table 1 shows the optimum sampling intervals for different filter lengths. Not surprisingly, the optimum sampling interval is smaller for longer filter lengths.

(e) Use the optimum sampling intervals, shown in Table 1, and equation (5) to obtain J_1 filters for lengths 61, 121 and 241. The J_0 and J_1 filter coefficients for filter lengths 61, 121 and 241 can be obtained on application to the author. The sampling functions are:

e^{an}, a = 0.145 and n = −30–30 for filter length 61;
e^{an}, a = 0.115 and n = −60–60 for filter length 121;
e^{an}, a = 0.065 and n = −120–120 for filter length 241.

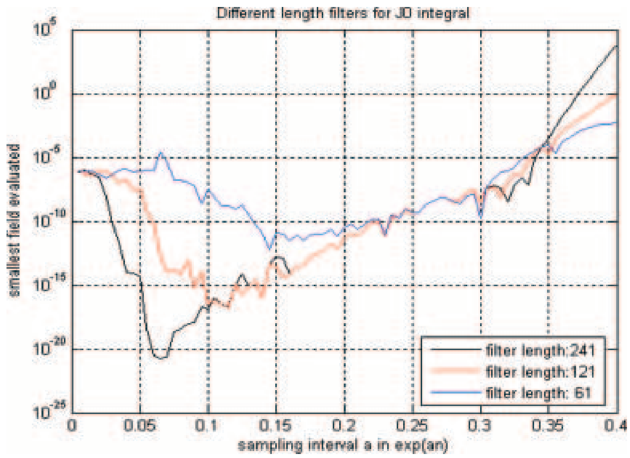

Figure 1 Smallest fields evaluated while varying the sampling interval for different filter lengths.

Table 1 Optimum sampling interval versus filter length

Filter length	61	121	241
Optimum sampling interval a	0.145	0.115	0.065

NEW FILTER PERFORMANCE TEST

For convenience, we use the following definitions

- Anders801: 801-point Anderson filters for J_0 and J_1 integrals (Anderson 1982);
- G & S120: 120-point Guptasarma and Singh filter for the J_0 integral (Guptasarma and Singh 1997);
- G & S140: 140-point Guptasarma and Singh filter for the J_1 integral (Guptasarma and Singh 1997);
- New61, New121 and New241: 61-point, 121-point and 241-point filters for the J_0 and J_1 integrals described here.

Guptasarma and Singh (1997) made a comprehensive comparison of many types of filter. From the comparison results for six known Hankel transforms, it has been shown that Anders801, G & S140 and G & S120 always perform the best and therefore we chose these three filters to compare with our filters. Another reason to choose Anders801 is that it is used in a well-known software package for modelling the field generated by a horizontal dipole in sea-bed CSEM (controlled-source electromagnetic) measurements, using the modelling code of Chave and Cox (1982), as referred to by MacGregor and Sinha (2000).

We use the Sommerfeld identity (equation 6) for the J_0 filter comparison, and the following equation (equation (B3), Chave and Cox 1982) for the J_1 filter comparison:

$$\int_0^\infty \mathrm{d}k J_1(k\rho)\frac{k^2}{\beta}\mathrm{e}^{-\beta|z-z'|} = \rho\frac{\mathrm{e}^{-\gamma R}}{R^3}(\gamma R + 1), \tag{7}$$

with parameters as defined in equation (6).

Fig. 2 compares the performances using the Sommerfeld identity (equation 6). It can be seen that our New61 has a similar performance to G & S120, in terms of the smallest field evaluated. New121 has a similar performance to Anders801. However, New121 and Anders801 can evaluate a smaller field (by a factor of 10^4) than New61 and G & S120. The performance of New241 is the best with another 10^5 improvement.

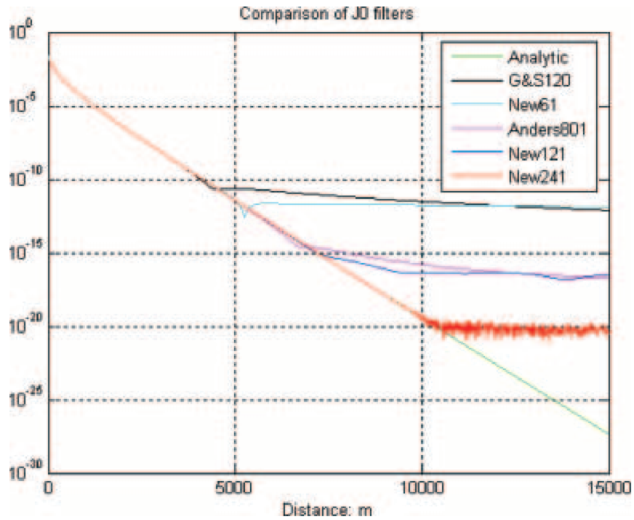

Figure 2 Comparison of J_0 filters for evaluating the Sommerfeld identity.

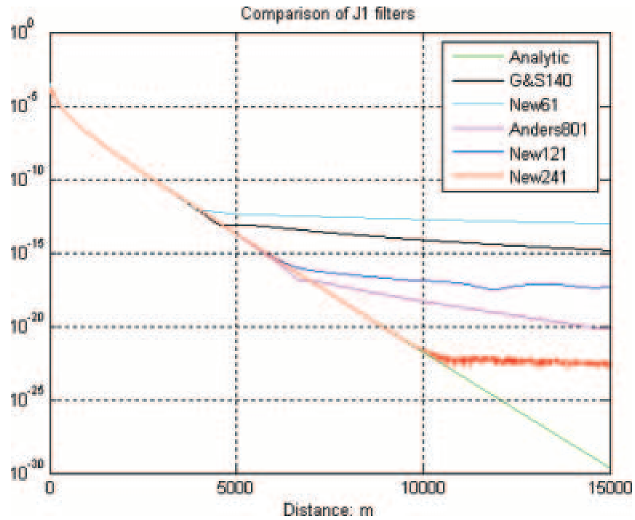

Figure 4 Comparison of J_1 filters for evaluating equation (7).

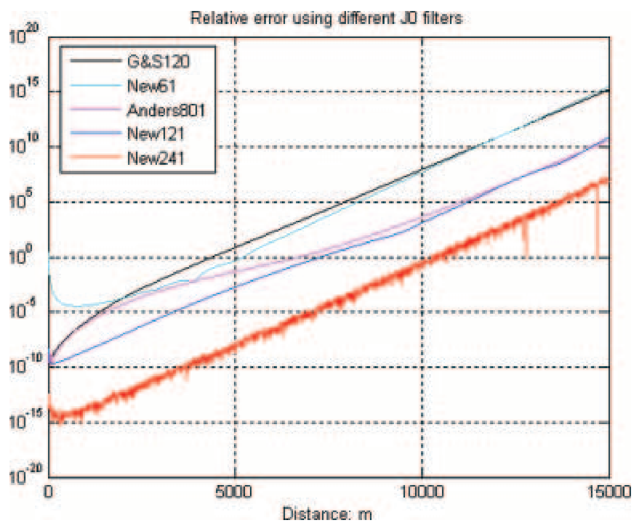

Figure 3 Relative errors using different J0 filters.

Note that Fig. 2 shows only the magnitudes of the complex fields.

Fig. 2 shows that all the filters can evaluate the fields very well within a distance of 4000 m. To examine the performance in detail, Fig. 3 shows the relative errors (relative to the theoretical value) for these filters.

Fig. 4 compares the results for J_1 filters. Comments on Fig. 4 are similar to those made for Fig. 2 above.

To evaluate the performance of the combined use of J_0 and J_1 filters, we use the equation for the in-line E-field (equation (30), Chave and Cox 1982), generated by a horizontal electric dipole placed in the sea ($\sigma = 3.2$ S/m):

$$E_\rho = \frac{IL}{4\pi\sigma}\left\{\int_0^\infty \mathrm{d}k\left(S(k\rho)\beta R_{\mathrm{TM}} - \frac{J_1(k\rho)}{\rho}\frac{\gamma^2}{\beta}R_{\mathrm{TE}}\right)\mathrm{e}^{-\beta(z+z')}\right.$$
$$\left. - \int_0^\infty \mathrm{d}k\left(J_0(k\rho)k\beta - \frac{J_1(k\rho)}{\rho}\frac{\gamma^2}{\beta}\right)\mathrm{e}^{-\beta|z-z'|}\right\}, \tag{8}$$

where I and L are the dipole current and length, Z and Z′ are, respectively, the receiver height (Z = 0) and the transmitter height (Z′ = 50 m) to the sea-bed with conductivity 1 S/m, $S(k\rho) = kJ_0(k\rho) - \frac{J_1(k\rho)}{\rho}$, and R^{TM} and R_{TE} are, respectively, the TM-wave and TE-wave reflection coefficients at the sea/sea–bed interface.

Fig. 5 compares results using the CSEM software to calculate the fields generated by a horizontal electrical dipole. The original software uses Anders801 to evaluate the combination of J_0 and J_1 integrals. We have now incorporated our filters into the software for comparison purposes. Although the analytical result is not known for this problem, it is known that in the far-field, the field decay rate is the same as that of the wave travelling in the homogeneous sea-bed material. Hence, the field magnitude versus distance will appear as a straight-line decay with a logarithmic *y*-axis, and the field will have a linear phase change for the far-field region. Based on this, we can see from Fig. 5(a) (magnitude) and Fig. 5(b) (phase) that the New241 filter performs very well up to the distance 15000 m where the E-field is as weak as 10^{-25} V/m. Using Anders801, the calculated field starts to contain errors at a distance of 11000 m (E-field: 10^{-21} V/m). The New61 and New121 can be used to calculate fields up to distances of 6000 m (E-field: 10^{-16} V/m) and 10000 m (E-field: 10^{-20} V/m), respectively.

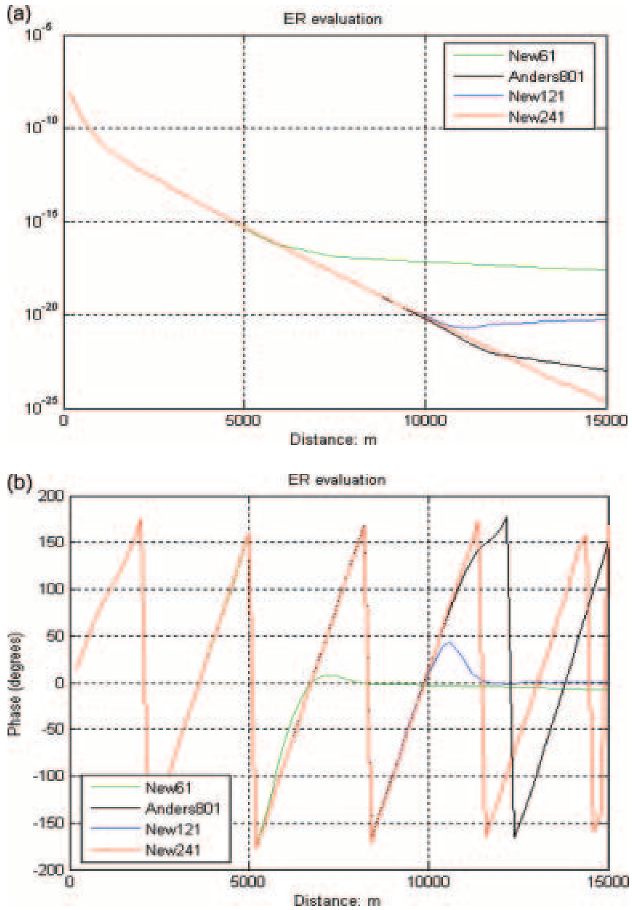

Figure 5 (a) Comparison of J_0 and J_1 filters for evaluating the magnitude of the E_R-field (equation 8). (b) Comparison of J_0 and J_1 filters for evaluating the phase of the E_R-field (equation 8).

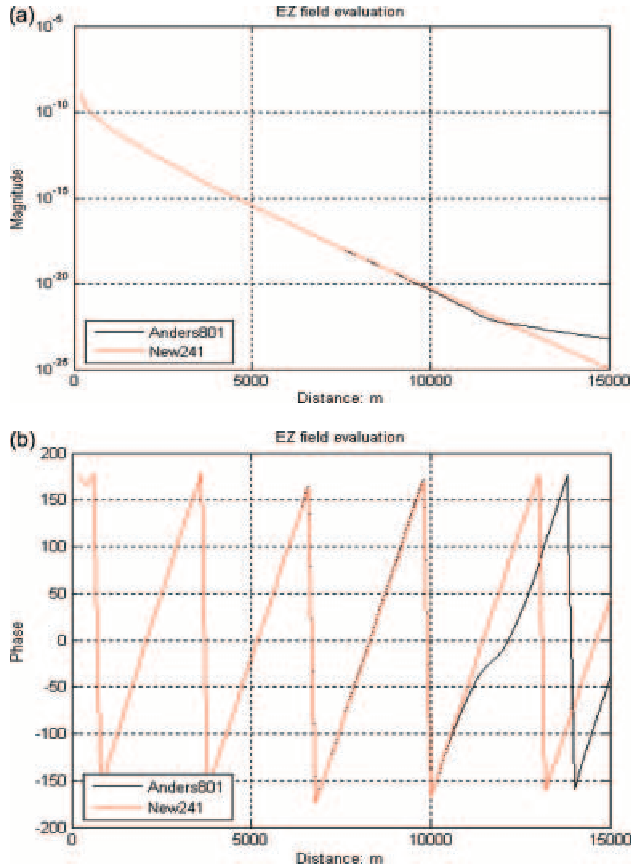

Figure 6 (a) Comparison of filters for evaluating the magnitude of the E_Z-field (equation 9). (b) Comparison of filters for evaluating the phase of the E_Z-field (equation 9).

The e-field in the z-direction (vertical) generated by a horizontal electrical dipole can be written (chave and cox 1982),

$$E_Z = -\frac{IL}{4\pi\sigma}\int_0^\infty \mathrm{d}k \mathrm{J}_1(k\rho)k^2\left(R_{\mathrm{TM}}\mathrm{e}^{-\beta(z+z')} + \mathrm{e}^{\beta(z-z')}\right). \qquad (9)$$

The results of the comparison between Anders801 and New241 for E_Z are shown in Figs 6(a.b).

DISCUSSION AND CONCLUSION

We have found a method to derive optimum filters for evaluating the Hankel transforms related to antenna radiation in a very conductive medium. Our New121 filter can evaluate weaker fields than G & S120 and G & S140 can, and our New241 filter can evaluate weaker fields than Anders80 can. Since the comparison is made for filters with different sampling intervals, it is not possible to say that our method is better than the methods used for obtaining G & S120, G & S140 and Anders801. We only say that for our particular application, use of our filters will save calculation time due to the short filter length and it will give better accuracy.

Christensen (1990, 1991) noted that the error decreases exponentially with the cut-off frequency. Hence, a moderate decrease in sampling interval will cause the error to decrease dramatically. Observing Fig. 1, our filters show the same behaviour although they are generated quite differently from Christensen's method. The smallest field evaluated decreases exponentially as the sampling interval is decreased over a certain range. However, Fig. 1 also shows that there is a limit to the increase in accuracy achieved by reducing the sampling interval. Beyond a certain point, reducing the sampling interval will reduce the accuracy. There is an optimum sampling interval for each filter length, the optimum sampling interval being smaller for longer filter lengths.

Table 2 shows a list of the sampling intervals for different filters. It is interesting to note that the sampling intervals of

Table 2 Sampling intervals for different filters

Authors	Filter length	Sampling interval
Koefoed *et al*. (1972)	47	0.23
Johanson (1975)	141	0.23
Nyman and Ladisman (1977)	31	0.22
Anderson (1979)	51	0.2
Anderson (1982)	801	0.1
Mohsen and Hashish (1994)	256	0.2
Guptasarma and Singh (1997)	47	0.25
Guptasarma and Singh (1997)	61	0.27
Guptasarma and Singh (1997)	120	0.21
Guptasarma and Singh (1997)	140	0.20

many published filters are around 0.2–0.25. This suggests that the sampling interval, as an optimization variable, should be further investigated in the future. Here, we only comment that in the sample-domain method, as in our method, there is no additional cost when using a small sampling interval. The calculation time for evaluating a Hankel transform is only related to the filter length, not to the sampling interval.

We use direct matrix inversion to solve the convolution equation (3). Compared to another type of sample-domain method, i.e. the Wiener–Hopf method (Koefoed and Dirks 1979; Guptasarma 1982; Guptasarma and Singh 1997), our direct method is much simpler. Guptasarma (1982) noted that the advantage of his method of sample-domain optimization might be lost if the length of the filter were increased and that, in any case, his method would be too laborious for large filter lengths. Guptasarma and Singh (1997) also mentioned some complications in solving the Wiener equation. In our case, the deconvolution is simple and fast, and there is no problem in generating long filters. The optimization curve for filter length 241 (the black curve in Fig. 1) is obtained in only 8 s on a 2.4 GHz PC. It involves obtaining 80 filters of length 241 for 80 sampling intervals varying from 0.005 to 0.4 in steps of 0.005 and evaluating the Sommerfeld identity 80 times. Here, we should note that in our optimization, we use only one variable, i.e. the sampling interval, instead of two variables, i.e. the sampling interval and the shift of Guptasarma and Singh (1997). Investigation into the effect of sampling shift on our optimization is a task for the future. Other future tasks are to optimize the value c defined in equation (5) and to consider ‘nonsymmetric’ filters. For the present, we have only considered the ‘symmetric’ filter case, i.e. $n = -L$ to L.

The common feature of the wavefields in our application is that they decay exponentially in the far-field. We use the Sommerfeld identity to derive the optimum sampling interval, because it reproduces this common feature. This guarantees that the sampling intervals optimized by the Sommefeld identity, a J_0 integral, can be used to evaluate other Hankel integrals related to our application. This may also explain why our filters, which are optimized for our application, perform better than G & S120, G & S140 and Anders801 filters in solving our special problems. In principle, the sampling function for the J_1 filter should be optimized separately using, for example, equation (7). However, it is practical to have the same sampling function for both J_0 and J_1 filters, since calculating the dipole antenna radiation involves the evaluation of both J_0 and J_1 integrals, as shown in equation (8). From Figs 5 and 6, we can see that the J_1 filters generated by the present method work well.

Fig. 3 shows the phenomenon of the relative errors of our filters increasing exponentially with distance, for far-fields. This explains why the numerical results in Figs 2 and 4 fit the analytical results very well for shorter distances and, from a certain distance, why the numerical results flatten out. Due to this flattening, the minimization of the smallest signal over the total distance of 15000 m becomes equivalent to the minimization of the fields at the turning point where the fit starts to deteriorate. This must be true for the case with filter length 241, since the numerical curves are very flat after the turning point. An alternative optimization criterion can be to minimize the calculated field at which the relative error reaches a certain value. We have tested these optimization criteria when choosing a relative error of 0.2. Both optimization criteria yield the same optimum values of a.

ACKNOWLEDGEMENT

The author thanks the Norwegian Research Council, Hydro Oil&Energy and Statoil for financial support through the PETROMAKS project.

REFERENCES

Anderson W.L. 1979. Numerical integration of related Hankel transforms of orders 0 and 1 by adaptive digital filtering. *Geophysics* **44**, 1287–1305.

Anderson W.L. 1982. Fast Hankel transforms using related and lagged convolutions. *ACM Transactions on Mathematical Software* **8**, 344–368.

Anderson W.L. 1989. A hybrid fast Hankel transform algorithm for electromagnetic modelling. *Geophysics* **54**, 263–266.

Anderson W.L. 1991. Comment on ‘Optimized fast Hankel transform filter’ by Niels Boie Christensen. *Geophysical Prospecting* **39**, 445–447.

Chave A.D. and Cox C.S. 1982. Controlled electromagnetic sources for measuring electrical conductivity beneath the oceans: 1. Forward problem and modelling study. *Journal of Geophysical Research* **87**, 5327–5338.

Christensen N.B. 1990. Optimized fast Hankel transform filters. *Geophysical Prospecting* **38**, 545–558.

Christensen N.B. 1991. Reply to comments by Walter L. *Anderson. Geophysical Prospecting* **39**, 449–450.

Eidesmo T., Ellingsrud S., MacGregor L.M., Constable S., Sinha M.C., Johansen S., Kong F.N. and Westerdahl H. 2002. Sea-bed logging, a new method for remote and direct identification of hydrocarbon filled layers in deepwater areas. *First Break* **20** (3), 144–152.

Ellingsrud S., Eidesmo T., Johansen S., Sinha M.C., MacGregor L.M. and Constable S. 2002. Remote sensing of hydrocarbon layers by sea-bed logging (SBL): Results from a cruise offshore Angola. *The The Leading Edge* **21**, 972–982.

Ghosh D.P. 1971. The application of linear filter theory to the direct interpretation of geoelectrical resistivity sounding measurements. *Geophysical Prospecting* **19**, 192–217.

Guptasarma D. 1982. Optimisation of shorter digital filters for increasing accuracy. *Geophysical Prospecting* **30**, 501–514.

Guptasarma D. and Singh B. 1997. New digital linear filters for Hankel J_0 and J_1 transforms. *Geophysical Prospecting* **45**, 745–762.

Johansen H.K. 1975. An interactive computer/graphic-display- terminal system for interpretation of resistivity soundings. *Geophysical Prospecting* **23**, 449–458.

Johansen H.K. and Sorensen K.I. 1979. Fast Hankel transforms. *Geophysical Prospecting* **27**, 876–901.

Koefoed O. Ghosh D.P. and Polman G.J. 1972. Computation of type curves for electromagnetic depth sounding with a horizontal transmitting coil by means of a digital linear filter. *Geophysical Prospecting* **20**, 406–420.

Koefoed O. and Dirks F.J. 1979. Determination of resistivity sounding filters by the Wiener–Hopf least-squares method. *Geophysical Prospecting* **27**, 245–250.

Kong F.N., Westerdahl H., Ellingsrud S., Eidesmo T. and Johansen S. 2002. Seabed logging: a possible direct hydrocarbon indicator for deep-sea prospects using EM energy. *Oil and Gas Journal* **100**(19):.

MacGregor L. and Sinha M. 2000. Use of marine controlled-source electromagnetic sounding for sub-basalt exploration. *Geophysical Prospecting* **48**, 1091–1106.

Mohsen A.A. and Hashsh E.A. 1994. The fast Hankel transform. *Geophysical Prospecting* **42**, 131–139.

Nyman D.C. and Landisman M. 1977. VES dipole-dipole filter coefficients. *Geophysics* **42**, 1037–1044.

Sorensen K.I. and Christensen N.B. 1994. The fields from a finite electrical dipole – A new computational approach. *Geophysics* **59**, 864–880.